

# Lattice QCD at finite isospin density at zero and finite temperature.

J. B. Kogut

*Dept. of Physics, University of Illinois,  
1110 West Green Street, Urbana, IL 61801-3080, USA*

D. K. Sinclair

*HEP Division, Argonne National Laboratory,  
9700 South Cass Avenue, Argonne, IL 60439, USA*

## Abstract

We simulate lattice QCD with dynamical  $u$  and  $d$  quarks at finite chemical potential,  $\mu_I$ , for the third component of isospin ( $I_3$ ), at both zero and at finite temperature. At zero temperature there is some  $\mu_I$ ,  $\mu_c$  say, above which  $I_3$  and parity are spontaneously broken by a charged pion condensate. This is in qualitative agreement with the prediction of effective (chiral) Lagrangians which also predict  $\mu_c = m_\pi$ . Although this transition appears to be second order, it exhibits the scaling properties of a tricritical point rather than the expected mean field scaling, which indicates that the lattice spacing is large enough for lattice artifacts to affect the nature of this transition. We have also studied the restoration of  $I_3$  symmetry at high temperature for  $\mu_I > \mu_c$ . For  $\mu_I$  sufficiently large, this finite temperature phase transition appears to be first order. As  $\mu_I$  is decreased it becomes second order connecting continuously with the zero temperature transition.

## I. INTRODUCTION

Neutron stars are made of dense cold nuclear matter – hadronic matter at high baryon-number density and low temperature. Large nuclei can be considered as droplets of nuclear matter. The relativistic heavy-ion collisions now being observed at RHIC and the CERN heavy-ion program can produce hadronic matter at high temperature and finite baryon-number density. Nuclear matter also has a finite (negative) isospin ( $I_3$ ) density due to Coulomb interactions, and it has been suggested that at very high densities it would have a finite strangeness density. Hence it is of interest to study QCD at finite quark/baryon-number density, finite isospin density and finite strangeness density at both zero and finite temperature.

Finite density is customarily studied through the introduction of a chemical potential for the charge of interest in the action. Introducing a finite chemical potential for quark-number leads to a complex fermion determinant with a real part of indefinite sign, which precludes use of standard simulation methods which rely on importance sampling. If we include a finite chemical potential,  $\mu_I$ , for  $I_3$  in the absence of any quark-number chemical potential, the fermion determinant remains non-negative, and simulations are possible. Such simulations can determine the QCD phase structure on one surface in the phase diagram for nuclear matter. One can hope that this will identify phases which will persist to finite baryon/quark-number density, and determine their properties.

We have performed simulations of lattice QCD with 2 flavours of light staggered quarks at finite  $\mu_I$  for both zero and finite temperatures. Preliminary results of these simulations were reported at Lattice2001 [1]. We included a small explicit  $I_3$ -breaking interaction needed to observe spontaneous symmetry breaking on a finite lattice. In addition to allowing us to observe spontaneous breaking of  $I_3$  (and parity), this term renders the fermion determinant strictly positive. Our zero temperature simulations were performed on an  $8^4$  lattice at an intermediate value of the coupling constant. In the limit that our symmetry-breaking parameter vanishes, there is some  $\mu_I = \mu_c$  above which  $I_3$  and parity are broken spontaneously by a charged pion condensate. This is in accord with the predictions of Son and Stephanov using effective (chiral) Lagrangians [2]. However, we do not observe the mean-field scaling near  $\mu_c$  predicted by these effective Lagrangians. The scaling we observe

is consistent with tricritical behaviour which we attribute to the coarseness of the lattice. We expect that mean field scaling would be seen at weaker couplings. These results are similar to those obtained in studies of the quenched version of this theory [3]. They are also similar to what is observed for 2-colour QCD at finite chemical potential  $\mu$  for quark-number [4, 5]. This is not surprising since the effective Lagrangian analysis of 2-colour QCD at finite  $\mu_I$  [6] is similar to that for QCD at finite  $\mu_I$ .

Our finite temperature simulations were performed on  $8^3 \times 4$  lattices. At sufficiently high temperature and  $\mu_I > \mu_c$ , we observe the evaporation of the symmetry-breaking pion condensate. For  $\mu_I$  sufficiently large, this transition is first order. As  $\mu_I \rightarrow \mu_c$  this transition softens and appears to become second order. Such a transition from first to second order should occur at a tricritical point. Again these results are similar to what we observed for 2-colour QCD at finite quark-number chemical potential [7].

Section 2 gives details of the actions and their symmetries. In section 3 we present our zero temperature results and scaling analyses. The finite temperature results are presented in section 4. Discussions, conclusions and an outline of planned extensions are given in section 5.

## II. LATTICE ACTION AND SYMMETRIES

The staggered fermion part of the action for lattice QCD with degenerate  $u$  and  $d$  quarks at a finite chemical potential  $\mu_I$  for isospin ( $I_3$ ) is

$$S_f = \sum_{sites} \bar{\chi} [\not{D}(\tau_3 \mu_I) + m] \chi \quad (1)$$

where  $\not{D}(\mu)$  is the standard staggered  $\not{D}$  with links in the  $+t$  direction multiplied by  $e^{\frac{1}{2}\mu}$  and those in the  $-t$  direction multiplied by  $e^{-\frac{1}{2}\mu}$  [3]. When  $\mu_I = m = 0$ , this action has a global  $U(2) \times U(2)$  flavour symmetry under which

$$\begin{aligned} \chi &\longrightarrow \exp[i(\theta + \epsilon\phi) \cdot \tau] \chi \\ \bar{\chi} &\longrightarrow \bar{\chi} \exp[-i(\theta - \epsilon\phi) \cdot \tau] \end{aligned} \quad (2)$$

where  $\tau = (1, \vec{\tau})$ ,  $\theta$  and  $\phi$  are site-independent 4-component “vectors”, and  $\epsilon = \epsilon(x) = (-1)^{x+y+z+t}$ . Spontaneous symmetry breaking can occur in any direction in this space. If

we keep  $\mu_I = 0$  and allow  $m \neq 0$ , the symmetry is broken down to  $U(2)_V$ . On the other hand if we keep  $m = 0$  and allow  $\mu_I \neq 0$ , the symmetry is broken down to  $U(1) \times U(1) \times U(1) \times U(1)$  generated by  $1$ ,  $\tau_3$ ,  $\epsilon$  and  $\epsilon\tau_3$ . Finally in the general case where neither  $\mu_I$  nor  $m$  vanishes, the symmetry is reduced to  $U(1)_V \times U(1)_V$  associated with  $1$  and  $\tau_3$ .

In order to predict potential symmetry breaking patterns we make several simple modifications of the arguments of Son and Stephanov [2] to apply them to the staggered lattice action. The generic quark bilinear which creates a meson has the form

$$M = \bar{\chi}\Gamma\chi. \quad (3)$$

The propagator for such a meson obeys the inequality

$$|\langle M(x)M^\dagger(0) \rangle| \leq \text{const} \langle S(x,0)S^\dagger(x,0) \rangle. \quad (4)$$

Thus, meson operators  $M$  whose propagators are proportional to  $\langle S(x,0)S^\dagger(x,0) \rangle$ , are potential Goldstone bosons. Now we note that our Dirac operator obeys

$$\tau_{1,2}\epsilon[\not{D}(\tau_3\mu_I) + m]\epsilon\tau_{1,2} = [\not{D}(\tau_3\mu_I) + m]^\dagger, \quad (5)$$

so  $i\bar{\chi}\epsilon\tau_{1,2}\chi$  are Goldstone candidates. These are linear combinations of  $\pi^+$  and  $\pi^-$  creation operators which means that if spontaneous breaking of the remnant flavour symmetry should occur, one linear combination of  $\pi^\pm$  will become a Goldstone boson while the orthogonal linear combination will develop a vacuum expectation value – a charged pion condensate. We note, in passing, that in the limit of massless quarks

$$\tau_{1,2}\not{D}(\tau_3\mu_I)\tau_{1,2} = -\not{D}(\tau_3\mu_I)^\dagger, \quad (6)$$

and we have 2 additional Goldstone boson candidates,  $\bar{\chi}\tau_{1,2}\chi$ , and if spontaneous symmetry breaking does occur we will have 2 Goldstone bosons rather than 1.

Since, in order to observe spontaneous symmetry breaking on a finite lattice, one needs to add a small explicit symmetry breaking term in the direction defined by the condensate, we choose to work with the fermion action

$$S_f = \sum_{\text{sites}} [\bar{\chi}[\not{D}(\tau_3\mu_I) + m]\chi + i\lambda\epsilon\bar{\chi}\tau_2\chi] \quad (7)$$

where the term proportional to the (small) parameter  $\lambda$  serves this purpose. The Dirac operator now has the determinant

$$\det[\not{D}(\tau_3\mu_I) + m + i\lambda\epsilon\tau_2] = \det[\mathcal{A}^\dagger\mathcal{A} + \lambda^2] \quad (8)$$

where we have defined

$$\mathcal{A} \equiv \mathcal{D}(\mu_I) + m. \quad (9)$$

(Note that this is a  $1 \times 1$  matrix in the flavour space on which the  $\tau$ s act.) We see that adding this symmetry breaking term has the effect of rendering the determinant strictly positive, which enables us to use the hybrid molecular-dynamics (HMD) algorithm to simulate this theory. Note that this theory has 8 continuum flavours. We use the HMD method to take the required fourth root of the determinant reducing this to 2 continuum flavours. For the purpose of simulation, it is convenient to multiply the Dirac operator on the left by the matrix  $\text{diag}(1, -\epsilon)$  and on the right by the matrix  $\text{diag}(1, \epsilon)$ . The transformed matrix  $\widetilde{\mathcal{M}}$ , has the same determinant as the original Dirac operator, and  $\widetilde{\mathcal{M}}^\dagger \widetilde{\mathcal{M}}$  is block diagonal, with the upper and lower blocks having the same determinant. This means that we use ‘noisy’ fermions and generate Gaussian noise for both upper and lower components of  $\widetilde{\mathcal{M}}\dot{\chi}$ , but only keep the upper components of  $\dot{\chi}$  after the inversion. Thus we still have only 8 flavours in the quadratic formulation. This is completely analogous to the odd-even lattice separation which prevents further species doubling in staggered lattice QCD at zero chemical potential.

Quantities we measure include the chiral condensate,

$$\langle \bar{\psi}\psi \rangle \Leftrightarrow \langle \bar{\chi}\chi \rangle, \quad (10)$$

the charged pion condensate

$$i\langle \bar{\psi}\gamma_5\tau_2\psi \rangle \Leftrightarrow i\langle \bar{\chi}\epsilon\tau_2\chi \rangle \quad (11)$$

and the isospin density

$$j_0^3 = \frac{1}{V} \left\langle \frac{\partial S_f}{\partial \mu_I} \right\rangle. \quad (12)$$

Here we have included both the lattice and continuum versions of the condensates. To get this simple continuum form for the charged pion condensate requires absorbing a factor of  $\xi_5$  (the flavour analogue of  $\gamma_5$ ) into the definition of the  $d$ -quark field.

### III. LATTICE SIMULATIONS AT ZERO TEMPERATURE

We have simulated  $N_f = 2$  lattice QCD at finite  $\mu_I$  on an  $8^4$  lattice at an intermediate coupling  $\beta = 6/g^2 = 5.2$ . This  $\beta$  was chosen since it represents an approximate lower bound to estimates of the finite temperature transition value for  $N_t = 4$  in the chiral limit. This

was used to keep finite volume effects at acceptable levels. We performed simulations at 2 different quark masses ( $m = 0.025$  and  $m = 0.05$ ) to see that varying the mass did not affect the qualitative behaviour of the theory and that we understood the effects of changing the quark mass.

At  $m = 0.025$ , we performed runs, each of 2000 molecular-dynamics time units in length, at 17 different  $\mu_I$  values ( $0 \leq \mu_I \leq 2$ ) for each of  $\lambda = 0.0025$  and  $\lambda = 0.005$ . Using 2  $\lambda$  values, both chosen to be much less than  $m$ , enabled us to extrapolate to the  $\lambda = 0$  limit, which is our ultimate interest. (We also ran at  $\mu_I = 3.0$ ,  $\lambda = 0.005$  to check saturation.)

The charged pion condensates,  $i\langle\bar{\psi}\gamma_5\tau_2\psi\rangle$  from these simulations are presented in figure 1 as functions of  $\mu_I$ , along with a linear extrapolation to  $\lambda = 0$ . This extrapolation strongly suggests that the  $\lambda \rightarrow 0$  condensate vanishes for  $\mu_I < \mu_c \sim 0.3 - 0.4$ , above which it is finite. This would indicate a phase transition to a phase in which  $I_3$  symmetry is broken spontaneously by a charged pion condensate, with an associated Goldstone mode.

This behaviour is predicted by the effective (chiral) Lagrangian analyses of Son and Stephanov, which also predict that the transition should be second order with mean-field exponents [2]. We fit our extrapolated ‘data’ to the critical scaling form

$$i\langle\bar{\psi}\gamma_5\tau_2\psi\rangle = \text{const} (\mu_I - \mu_c)^{\beta_m} \quad (13)$$

for  $\mu_I > \mu_c$  close to the transition. Fitting to this form over the range  $0.4 \leq \mu_I \leq 1.0$ , we find  $\mu_c = 0.394(1)$ ,  $\beta_m = 0.230(9)$  and  $\text{const} = 1.23(2)$  at a 62% confidence level. This is clearly inconsistent with mean field scaling for which  $\beta_m = \frac{1}{2}$ . It is, however, suggestive of tricritical scaling for which  $\beta_m = \frac{1}{4}$ .

The tricritical scaling form is (see for example [8])

$$i\langle\bar{\psi}\gamma_5\tau_2\psi\rangle = b\phi + (c/3)\phi^3, \quad (14)$$

where  $\phi(\mu_I, \lambda)$  is the solution of

$$\phi^5 - c\lambda\phi^2 - a(\mu_I - \mu_c)\phi - b\lambda = 0 \quad (15)$$

which is the global minimum of

$$(1/6)\phi^6 - (c/3)\lambda\phi^3 - (a/2)(\mu_I - \mu_c)\phi^2 - b\lambda\phi = 0. \quad (16)$$

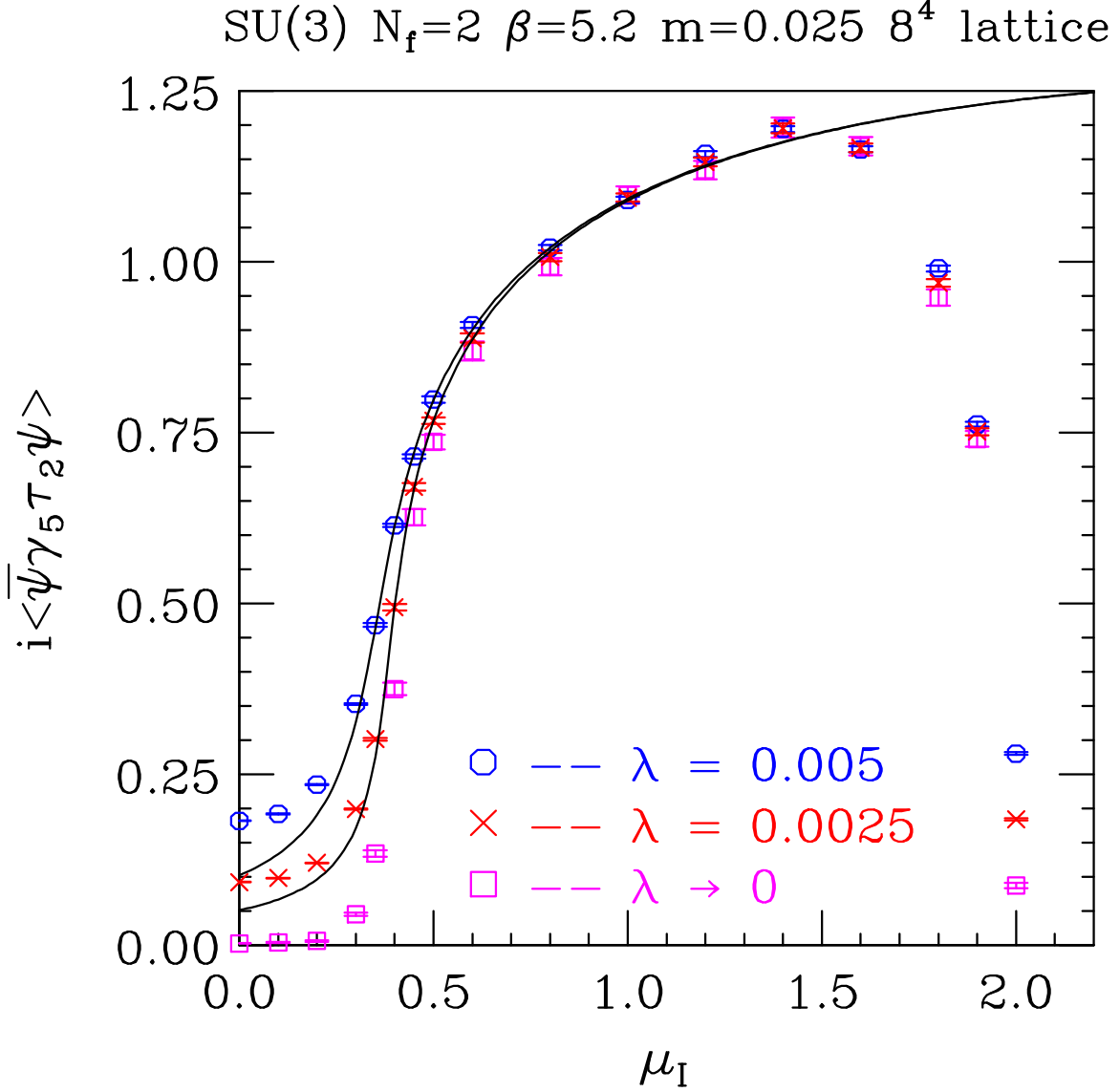


FIG. 1: Charged pion condensate as a function of  $\mu_I$  for  $\lambda = 0.0025$ ,  $\lambda = 0.005$  and  $\lambda \rightarrow 0$ . The curves are fits of the finite  $\lambda$  measurements to tricritical scaling.

Fitting our ‘data’ for both  $\lambda = 0.0025$  and  $\lambda = 0.005$  to this form over the range  $0.4 \leq \mu_I \leq 1.0$ , we obtain a fit with  $\mu_c = 0.426(3)$ ,  $a = 0.39(1)$ ,  $b = 1.85(2)$  and  $c = -1.8(1)$  at a 25% confidence level. This fit is shown as the 2 solid lines in our plot. We note that it provides a reasonable fit to the  $\mu_I > \mu_c$  results until saturation takes over around  $\mu_I = 1.5$ . The fall-off at large  $\mu_I$  is the effect of saturation, when the occupation number of each site becomes the maximum allowed by fermi statistics. As such it is a finite lattice spacing effect. This interpretation will become clearer when we present measurements of the isospin ( $I_3$ ) density.

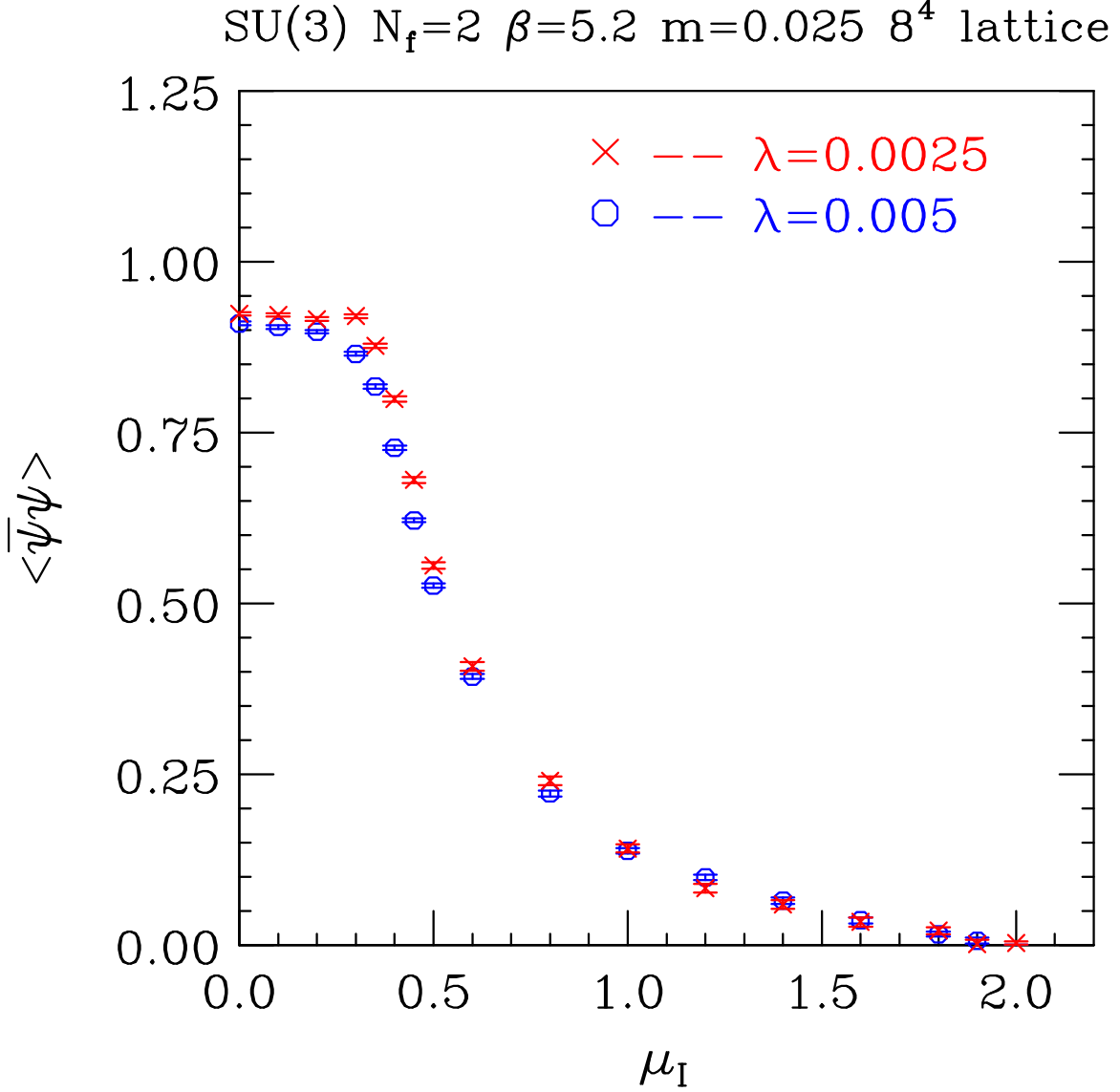


FIG. 2: Chiral condensate as a function of  $\mu_I$  for  $\lambda = 0.0025$  and  $\lambda = 0.005$ .

In figure 2 we present the chiral condensate for the same set of simulations. The general characteristics of these graphs are that  $\langle \bar{\psi}\psi \rangle$  remains roughly constant for  $\mu_I < \mu_c$ , after which it drops rapidly, approaching zero at large  $\mu_I$ . Although this can qualitatively be thought of as the condensate rotating from the chiral to the isospin-breaking direction, it is not a simple rotation, since the magnitude of the total condensate increases up until saturation effects take over. This contrasts with the predictions of lowest order effective Lagrangians where it is a simple rotation. However, in the case of 2-colour QCD at finite quark-number chemical potential, whose effective Lagrangian is structurally very similar to that for the theory at hand, the effective Lagrangian/chiral perturbation theory calculations

have been extended to next-to-leading order [9]. Here, although mean field scaling survives, the rotation of the condensate is accompanied by a rescaling. We suspect that the qualitative features of this analysis will apply to the effective Lagrangian approach to QCD at finite  $\mu_I$ .

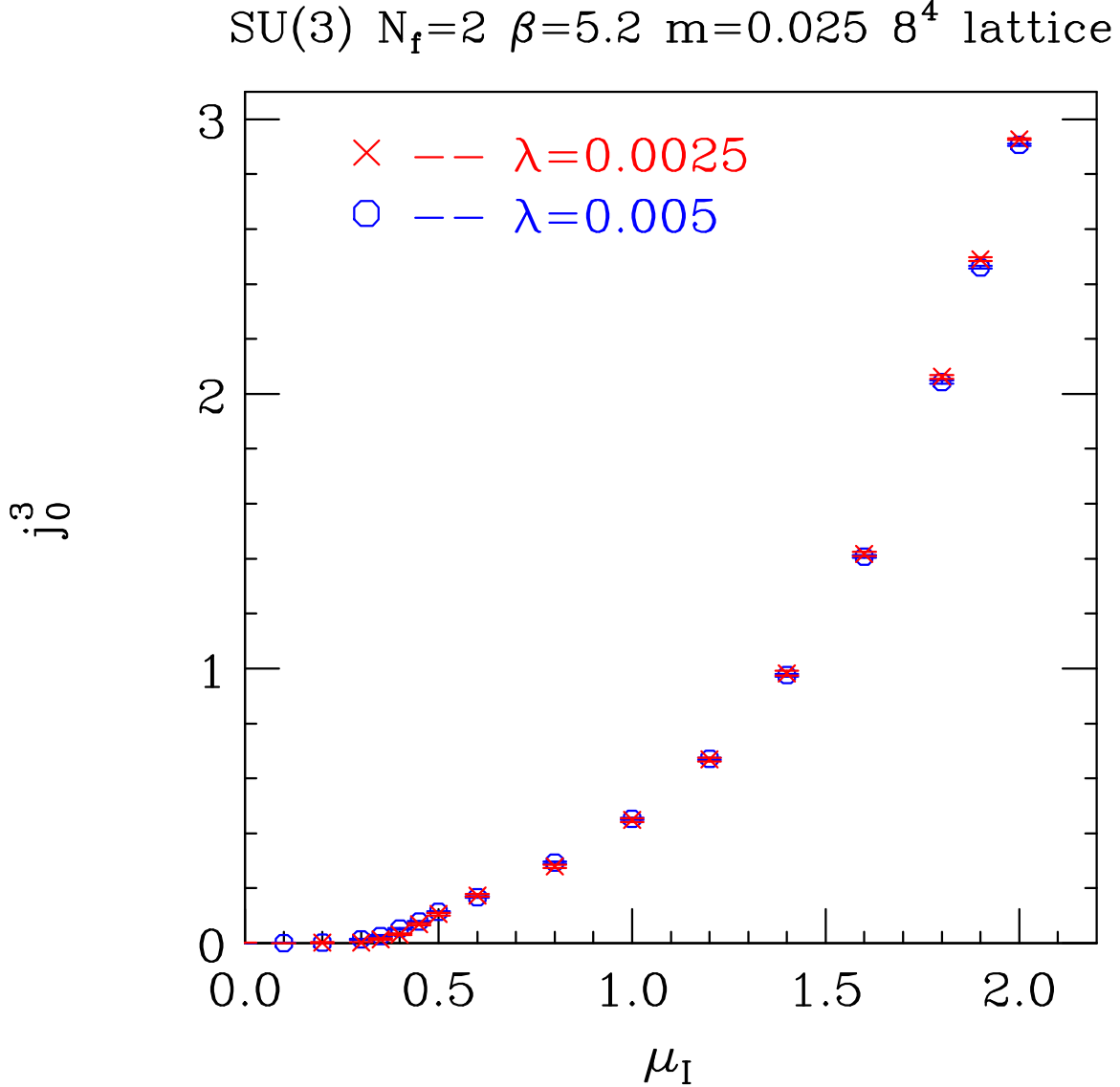


FIG. 3: Isospin( $I_3$ ) density as a function of  $\mu_I$  for  $\lambda = 0.0025$  and  $\lambda = 0.005$ .

Figure 3 presents the isospin ( $I_3$ ) density as a function of  $\mu_I$ . While the 2 condensates are normalized to 4 flavours for comparison with previous ( $\mu_I = 0$ ) simulations,  $j_0^3$  is normalized to 8 flavours, which is the natural normalization for staggered quarks. Qualitatively, we note that  $j_0^3$  is close to zero for  $\mu_I < \mu_c$ , rises slowly (in comparison with the pion condensate) up to  $\mu_I \sim 1$ , after which it starts to rise more rapidly reaching its saturation value of 3 (1/2 for each of 3 colours and 2 ‘flavours’ per site) due to fermi statistics, at

$\mu_I \sim 2$ . (In fact measurements made at  $\mu_I = 3.0$  give a value consistent with 3). Saturation is clearly a finite lattice spacing effect and hence requires no further discussion. We also note that there is very little  $\lambda$  dependence. To study critical scaling, we have fitted  $j_0^3$  to the form

$$j_0^3 = \text{const} (\mu_I - \mu_c)^{\beta_I} \quad (17)$$

for  $\mu_I > \mu_c$ . Fits over the range  $0.4 \leq \mu_I \leq 0.8$  give  $\beta_I = 0.80(5)$  ( $\mu_c = 0.372(7)$ ,  $\text{const} = 0.55(2)$ ) at a 51% confidence level for  $\lambda = 0.0025$ , and  $\beta_I = 1.07(8)$ , ( $\mu_c = 0.30(2)$ ,  $\text{const} = 0.62(2)$ ) at a 26% confidence level for  $\lambda = 0.005$ . These appear consistent with the value  $\beta_I = 1$  for the mean-field predictions of Son and Stephanov.

As also noted by Son and Stephanov, measuring  $j_0^3$  as a function of  $\mu_I$  at  $T = 0$  and constant volume (since  $\beta$  is constant) yields the pressure  $p$  and energy density  $\epsilon$  as functions of  $\mu_I$ , since

$$p = \int_{\mu_c}^{\mu_I} j_0^3 d\mu_I \quad (18)$$

$$\epsilon = \int_0^{j_0^3} \mu_I dj_0^3 \quad (19)$$

for  $\mu_I > \mu_c$  and zero for  $\mu_I < \mu_c$ . In the region where equation 17 is valid, assuming  $\beta_I = 1$  these yield

$$p = \frac{1}{2} \text{const} (\mu_I - \mu_c)^2 \quad (20)$$

$$\epsilon = \text{const} \mu_c (\mu_I - \mu_c) \quad (21)$$

$$\frac{p}{\epsilon} = \frac{1}{2} \left( \frac{\mu_I}{\mu_c} - 1 \right) \quad (22)$$

where we have kept only the leading order in  $(\mu_I - \mu_c)$  in each of these expressions. The last of these equations is a form of the equation of state for this system in the neighbourhood of  $\mu_c$ . Clearly we could extend each of these expressions beyond the scaling region by interpolating the ‘data’ of figure 3 and performing the relevant integrals analytically or numerically.

We performed similar simulations at the same coupling  $\beta = 5.2$  and mass  $m = 0.05$  at  $\lambda = 0.005$  and  $\lambda = 0.01$ . Here we concentrated on the neighbourhood of the phase transition and used more closely spaced (in  $\mu_I$ ) points with somewhat lower statistics. Again we were able to fit our ‘data’ for the pion condensate to a tricritical scaling function, this time to the simpler form with  $c$  set to zero in the above analysis. Fitting over the range

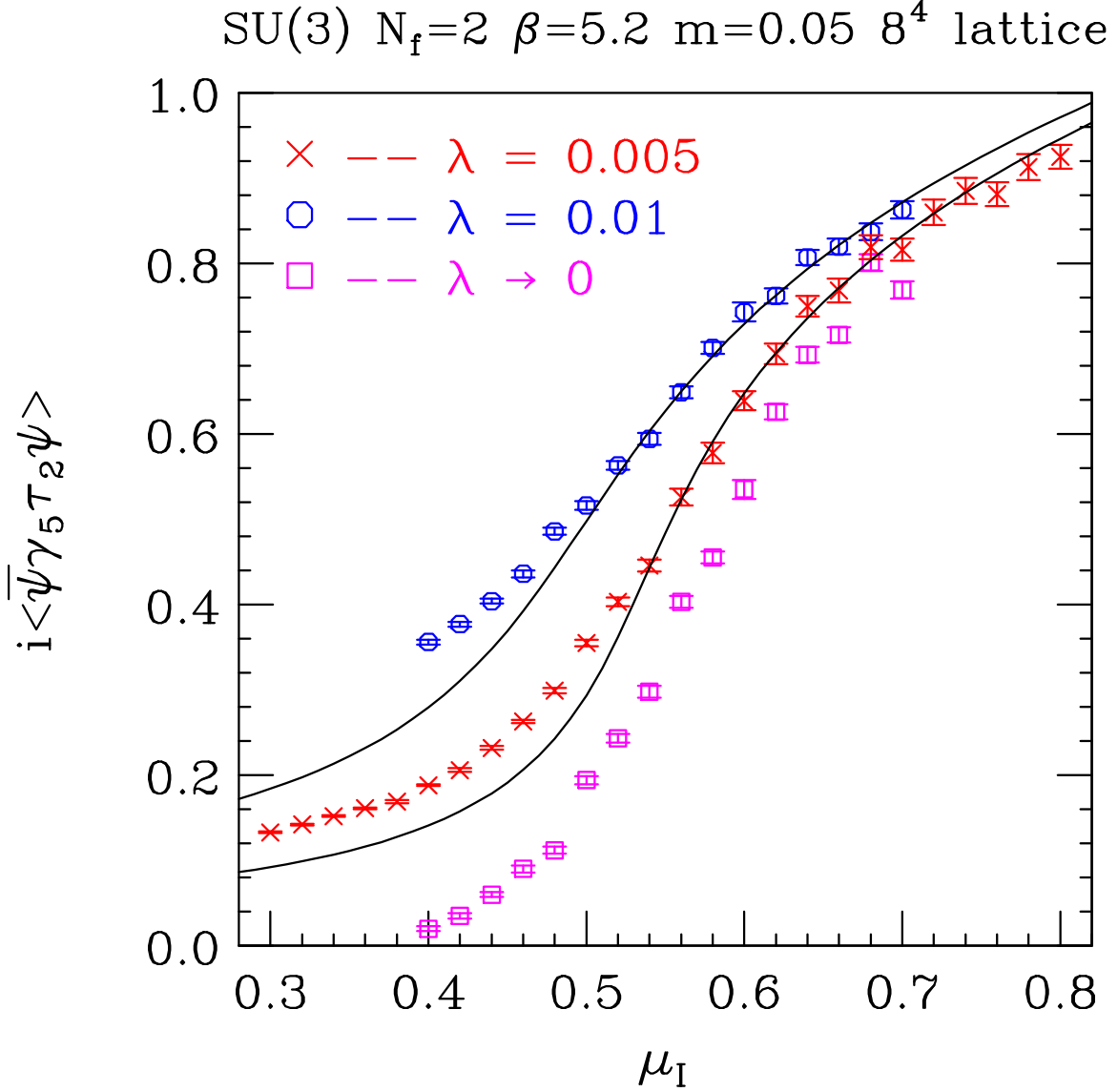


FIG. 4: Pion condensates as functions of  $\mu_I$  for  $\lambda = 0.005$ ,  $\lambda = 0.01$  and a linear extrapolation to  $\lambda = 0.0$ . The lines are the tricritical fit described in the text.

$0.54 \leq \mu_I \leq 0.70$ , we obtained a fit with  $\mu_c = 0.588(4)$ ,  $a = 0.49(2)$  and  $b = 1.62(2)$  at a 40% confidence level. Not only do we see qualitative consistency with the smaller mass results, but when systematic errors are taken into account, our measured values of  $\mu_c$  are consistent with the expectation that  $\mu_c(m = 0.05) = \sqrt{2}\mu_c(m = 0.025)$  which would be true if, indeed,  $\mu_c = m_\pi$ , from PCAC. This ‘data’ for the pion condensate with the scaling fits superimposed is plotted in figure 4.

#### IV. SIMULATIONS AT FINITE TEMPERATURE

We have performed simulations of QCD at finite  $\mu_I$  and finite temperature on an  $8^3 \times 4$  lattice, with  $m = 0.05$ . Most of these simulations were performed at  $\lambda = 0.005$  and  $\lambda = 0.01$ , i.e.  $\lambda \ll m$ , with the objective of obtaining information about the  $\lambda = 0$  limit. The goal of these simulations is to map out the region of the  $(\beta, \mu_I)$  and hence the  $(T, \mu_I)$  plane where  $I_3$  is spontaneously broken by a charged pion condensate, and determine the nature of the phase transitions which demarcate its boundaries.

The first of these simulations was performed at a fixed, large (but well below saturation) value of  $\mu_I$ . The value chosen was  $\mu_I = 0.8$ . At  $\beta$  low enough to approximate zero temperature on an  $N_t = 4$  lattice, the system is in the phase where  $I_3$  is spontaneously broken by a (large) pion condensate. As  $\beta$  is increased we eventually reach a value  $\beta = \beta_c$  at which this condensate evaporates. For  $\beta > \beta_c$  we are in the phase where the pion condensate vanishes for  $\lambda \rightarrow 0$  and  $I_3$  is unbroken. A single  $\lambda$  value,  $\lambda = 0.005$  was used for these runs.

Figure 5 shows the  $\beta$  dependence of the pion condensate for these simulations. We see that for  $\beta \leq 5.2$  the condensate is large. Between  $\beta = 5.2$  and  $\beta = 5.3$  the condensate drops by an order of magnitude, and is small enough for  $\beta \geq 5.3$  that we are safe to assume that it would vanish in the  $\lambda \rightarrow 0$  limit. This drop is so precipitous that we suspect that it is first order, although we really need a larger lattice to confirm this.

We have also measured the Thermal Wilson Line (Polyakov Loop) during these runs. These measurements are shown in figure 6. For  $\beta \leq 5.2$ , the Wilson line is small indicating confinement. For  $\beta \geq 5.3$ , the Wilson line becomes large indicating deconfinement. The jump between  $\beta = 5.2$  and  $\beta = 5.3$  is again great enough to suggest a first order transition. This behaviour of the Wilson Line indicates that this is the temperature-driven deconfinement transition.

We have also run simulations on an  $8^3 \times 4$  lattice with  $\beta = 4.0$  which gives us the low temperature behaviour. We chose  $m = 0.05$  again and ran at  $\lambda = 0.005$  and  $\lambda = 0.01$  for  $0.20 \leq \mu_I \leq 2.0$  which covers both the transition from the  $I_3$  symmetric phase to the phase where  $I_3$  is spontaneously broken, and the approach to saturation. Our measurements of the pion condensate are shown in figure 7. Not surprisingly this graph resembles those we obtained on an  $8^4$  lattice since at  $\beta = 4.0$ , this lattice is essentially at zero temperature.

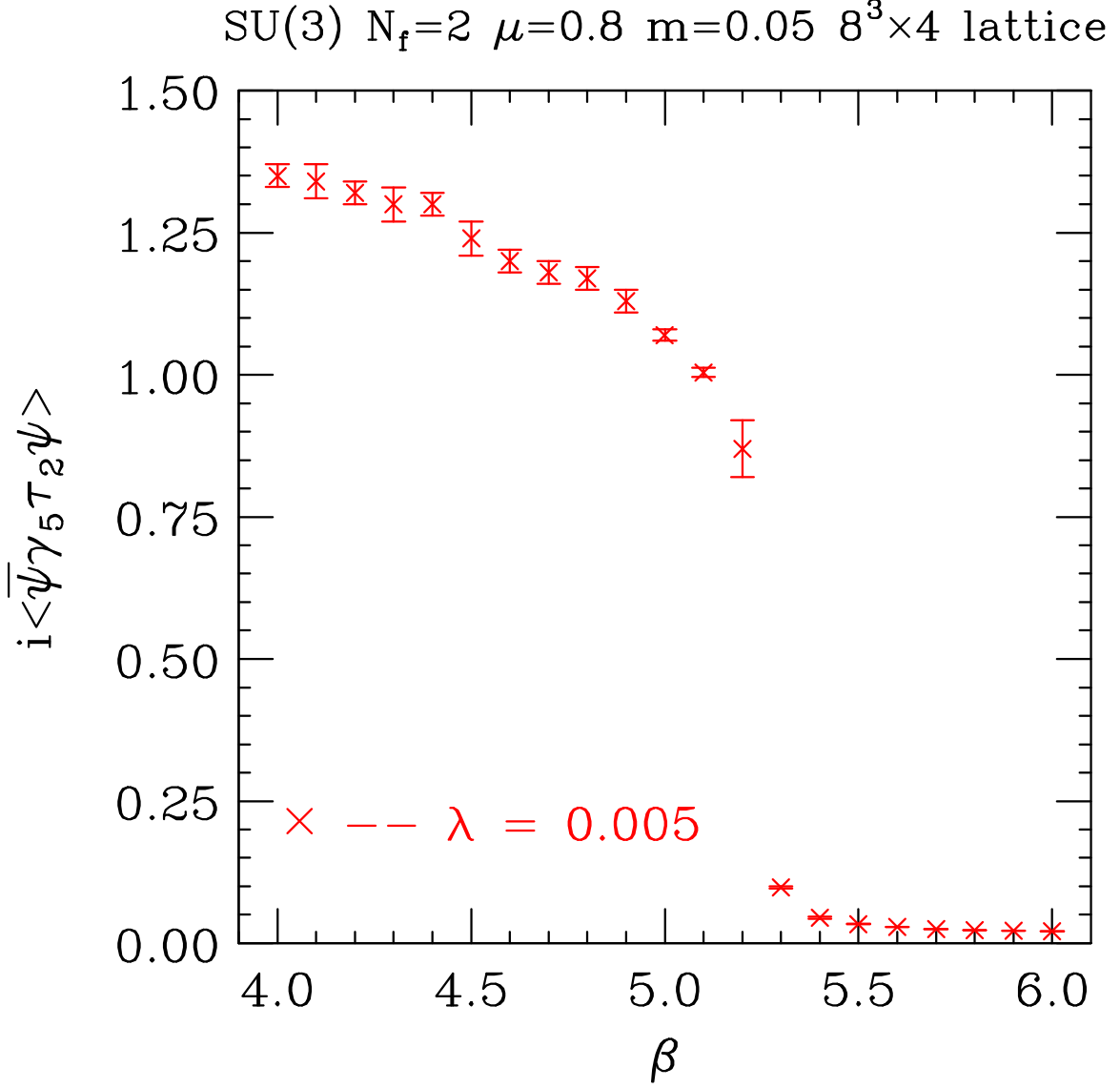


FIG. 5: Pion condensate as a function of  $\beta$  for  $m = 0.05$ ,  $\lambda = 0.005$ , and  $\mu_I = 0.8$  on an  $8^3 \times 4$  lattice.

Again we were able to fit the scaling behaviour near the transition to a tricritical form. The fit over the range  $0.55 \leq \mu_I \leq 0.8$  and both  $\lambda$  values yields a fit with  $\mu_c = 0.566(7)$ ,  $a = 0.73(7)$ ,  $b = 2.79(8)$ ,  $c = -4.7(6)$  and a confidence level of 48%. These fits are also shown in the figure.

In figure 8 we present the isospin density from these runs.  $j_0^3$  rises from zero at  $\mu_I \sim \mu_c$ . Again there is little  $\lambda$  dependence. The predicted linear scaling is clear on inspecting these graphs. This is born out by the fits. Fitting the  $\lambda = 0.005$  ‘data’ over

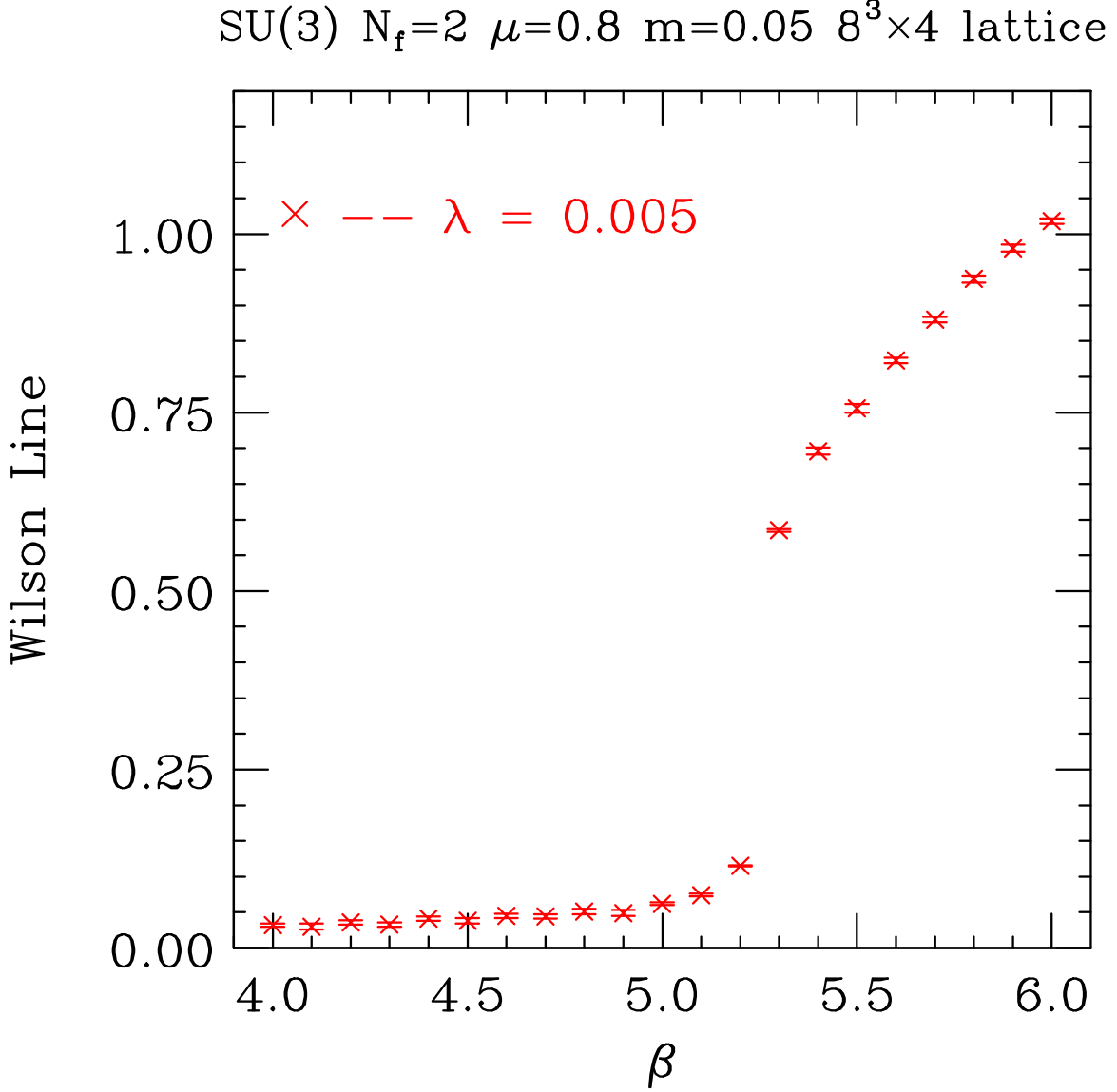


FIG. 6: Wilson linear a function of  $\beta$  for  $m = 0.05$ ,  $\lambda = 0.005$ , and  $\mu_I = 0.8$  on an  $8^3 \times 4$  lattice.

the range  $0.5 \leq \mu_I \leq 1.1$  gives  $\mu_c = 0.467(13)$ ,  $\beta_I = 0.94(6)$  and  $const = 1.22(3)$  at a confidence level of 18% while fitting the  $\lambda = 0.01$  ‘data’ yields  $\mu_c = 0.382(9)$ ,  $\beta_I = 1.09(3)$ ,  $const = 1.20(1)$  at a confidence level of 85%. These results are in excellent agreement with the effective Lagrangian prediction  $\beta_I = 1$ . This graph also indicates a crossover to a more rapid increase at  $\mu_I \sim 1.5$ .

Finally we have performed  $m = 0.05$  simulations on an  $8^3 \times 4$  lattice at  $\beta = 5.0$ , which lies below  $\beta_c$  at high  $\mu_I$ , while being large enough that the effects of finite temperature should be apparent. Here again we ran with  $\lambda = 0.005, 0.01$ . Here we used higher statistics (2000

SU(3)  $N_f=2$   $\beta=4.0$   $m=0.05$   $8^3 \times 4$  lattice

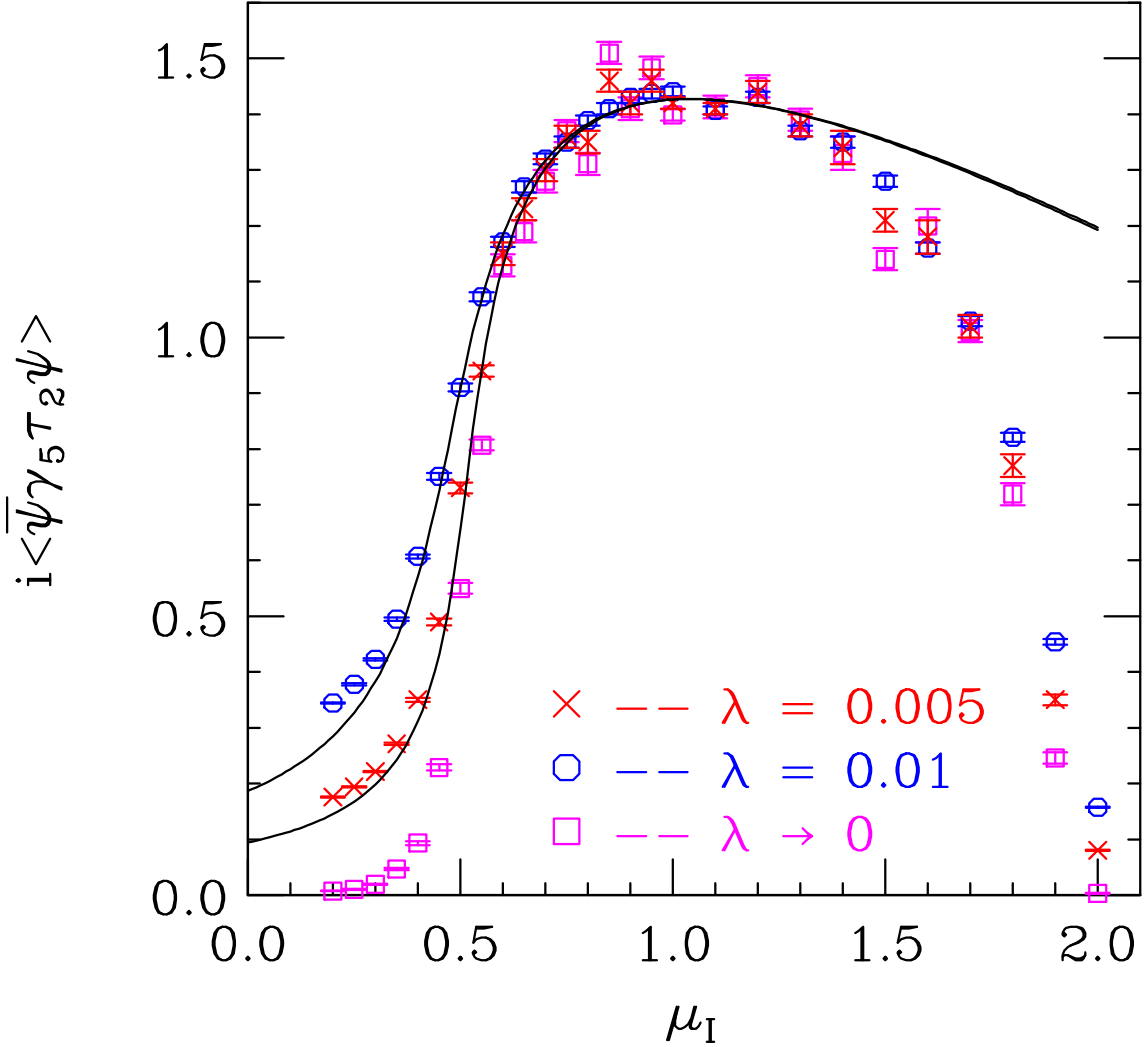


FIG. 7: Pion condensates as functions of  $\mu_I$  for  $\lambda = 0.005$ ,  $\lambda = 0.01$  and a linear extrapolation to  $\lambda = 0.0$  on an  $8^3 \times 4$  lattice at  $\beta = 4.0$ . The lines are the tricritical fit described in the text.

time-units per ‘run’) but at fewer  $\mu_I$  values. Our measurements of the charged pion condensate are presented in figure 9. The transition from low to high values of this condensate shows no sign of a first order transition. The linear extrapolation to  $\lambda = 0$  gives values close to zero at low  $\mu_I$ , rising rapidly from zero above some  $\mu_c \sim 0.5$ . Again we obtain an acceptable fit to tricritical scaling for both  $\lambda$  values over the range  $0.55 \leq \mu_I \leq 0.80$ , with  $\mu_c = 0.581(3)$ ,  $a = 0.55(2)$ ,  $b = 2.03(4)$  and  $c = -1.9(3)$  at a 28% confidence level, and note that extending this to include  $\mu_I = 0.90$  gives a fit with parameters consistent with these at a 16% confidence level. Clearly having more points within this range of  $\mu_I$  would have been

SU(3)  $N_f=2$   $\beta=4$   $m=0.05$   $8^3 \times 4$  lattice

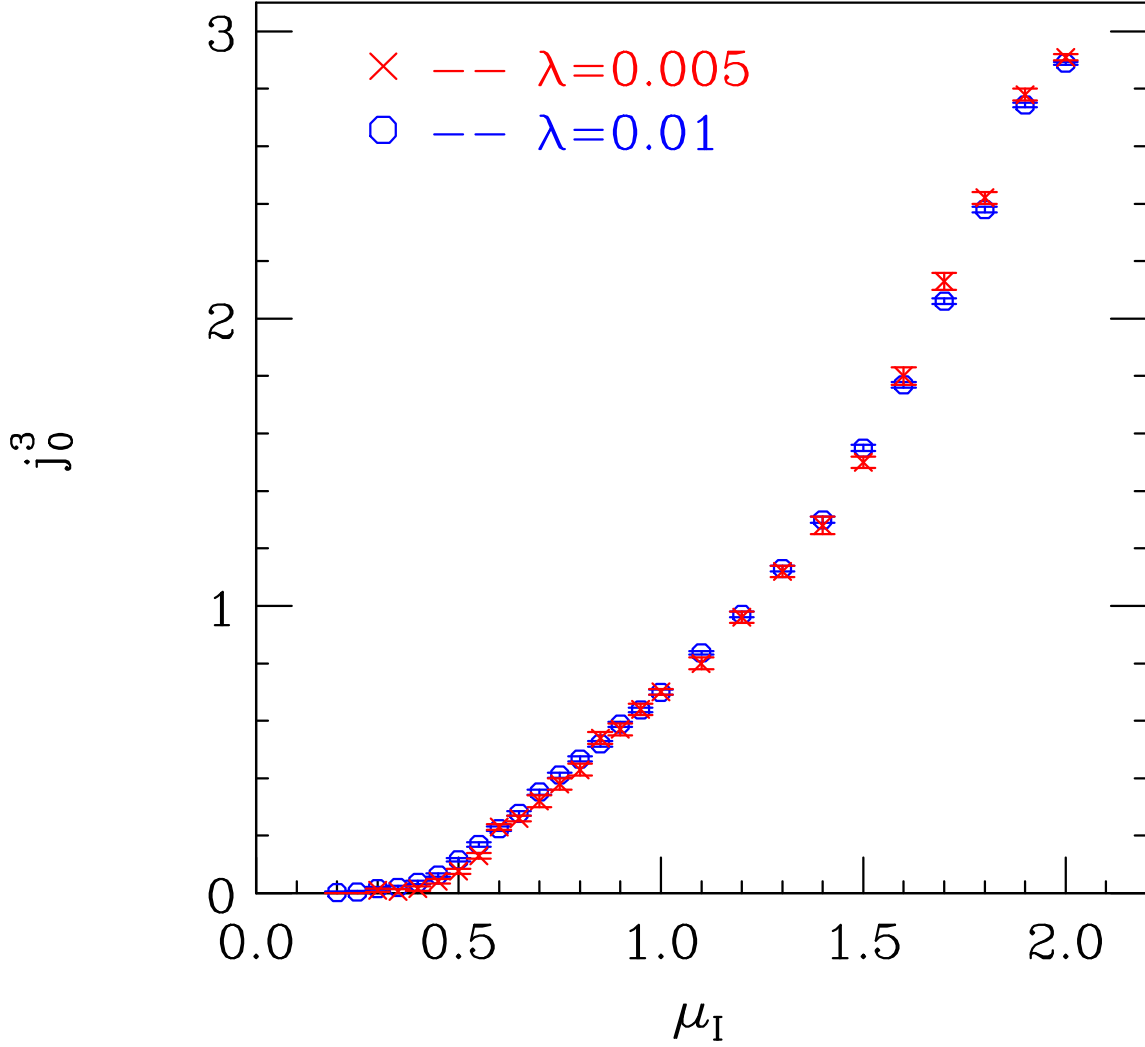


FIG. 8: Isospin( $I_3$ ) density as a function of  $\mu_I$  for  $m = 0.05$ ,  $\lambda = 0.005$  and  $\lambda = 0.01$  on an  $8^3 \times 4$  lattice at  $\beta = 4.0$ .

advantageous.

Thus the line of phase transitions which bound the region in the  $(\mu_I, T)$  plane within which isospin ( $I_3$ ) is broken spontaneously by a charged pion condensate, is second order for low temperatures and becomes first order at high  $\mu_I$ . Our experience with the quenched theory, and with 2-colour QCD at finite quark-number chemical potential leads us to believe that the fact that the second order transitions appear to be tricritical is an artifact of the coarse lattice, and that the expected mean field behaviour would occur at higher  $\beta$  values

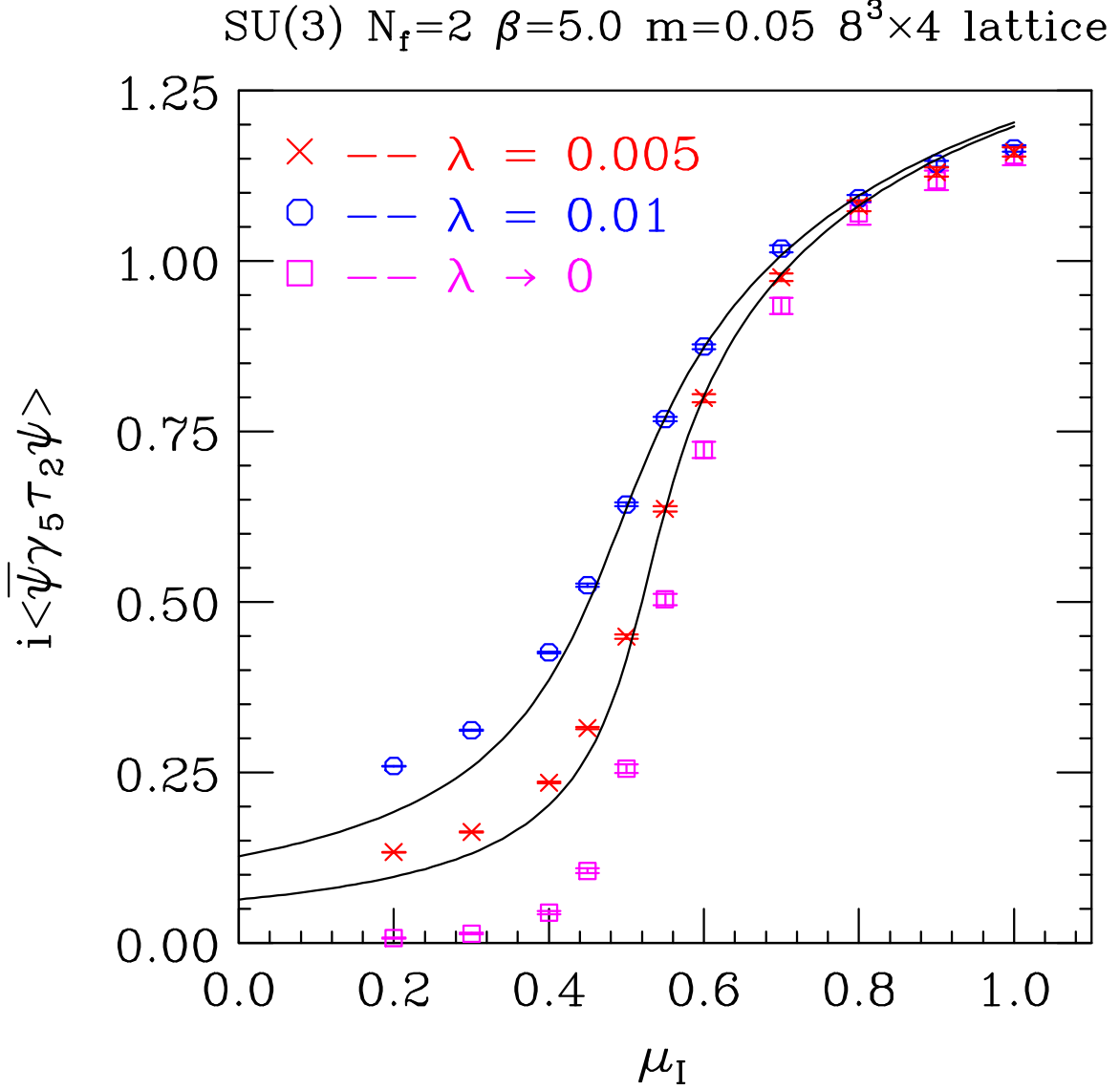


FIG. 9: Pion condensates as functions of  $\mu_I$  for  $\lambda = 0.005$ ,  $\lambda = 0.01$  and a linear extrapolation to  $\lambda = 0.0$  on an  $8^3 \times 4$  lattice, at  $\beta = 5.0$ . The lines are the tricritical fit described in the text.

which, in these finite temperature simulations, would require working with a lattice with larger  $N_t$ .

## V. DISCUSSION AND CONCLUSIONS

We have simulated QCD with 2 quark flavours ( $u, d$ ) at a finite chemical potential ( $\mu_I$ ) for isospin,  $I_3$ . At zero temperature and intermediate coupling ( $\beta = 6/g^2 = 5.2$ ) we found

strong evidence for a second order transition to a phase in which  $I_3$  is spontaneously broken by a charged pion condensate which also breaks parity, at  $\mu_I = \mu_c$ . Measurement of the scaling of this condensate close to the critical point ( $\mu_c$ ) indicates that it is a tricritical point rather than the mean field fixed point suggested by effective Lagrangian/chiral perturbation theory analyses. Our experience with 2-colour QCD [5] and with the quenched version [3] of this theory leads us to suspect that this tricritical behaviour is observed because at  $\beta = 5.2$ , finite lattice spacing artifacts are large enough to affect the nature of the transition, and that mean-field scaling would be observed for weak enough QCD couplings as is true for both the quenched theory and for 2-colour QCD at finite  $\mu$ . Aside from this, the observed behaviour is what is predicted by effective Lagrangian methods for  $\mu_I$  appreciably less than the value at which saturation, a lattice artifact, takes over. These effective Lagrangian analyses predict that  $\mu_c = m_\pi$ . Since we have not measured  $m_\pi$  on these small lattices, all we have checked is that  $\mu_c \propto \sqrt{m}$  for the 2 quark masses which we use ( $m = 0.025, m = 0.05$ ), and found that this is true within the uncertainties of our measurements.

We also measured the isospin density ( $j_0^3$ ) and found that it increases from zero, at or near  $\mu_c$ . The scaling behaviour appears to be linear close to  $\mu_c$ , as is predicted by effective Lagrangian analyses [2]. For larger  $\mu_I$  values it starts to increase considerably faster than linear. This is in qualitative agreement with the expectation that  $I_3$  density should increase as  $\mu_I^3$  at large  $\mu_I$ . We have not been able to determine if our observations are consistent with this  $\mu_I^3$  increase because of the effects of saturation which cause the isospin density to approach 3 at high  $\mu_I$ . Here we have indicated how the measurement of  $j_0^3$  enables one to obtain the pressure ( $p$ ) and the energy density ( $\epsilon$ ) as functions of  $\mu_I$ , and given explicit expressions for these quantities in the scaling regime.

The chiral condensate remains approximately constant for  $\mu_I < \mu_c$ . Above  $\mu_c$  it starts to fall approaching zero for large  $\mu$ . Again this is in agreement with expectations. However, the expectation from lowest-order effective Lagrangian tree-level analyses, that the chiral condensate simply rotates into the direction of the charged pion condensate, is not true. However, in closely related 2-colour QCD at finite quark-number chemical potential, chiral perturbation theory calculations through next-to-leading order show that, while scaling remains mean field, the condensate does not merely rotate, but also rescales [9]. Since the structure of chiral perturbation theory (effective Lagrangians) for the two

theories is so similar, we expect a similar result for QCD at finite  $\mu_I$ .

We have performed simulations at finite temperature ( $T$ ) in addition to finite  $\mu_I$ . In particular we have heated the system at fixed  $\mu_I = 0.8 > \mu_c(T = 0)$  (in lattice units) by increasing  $\beta$ . On our  $N_t = 4$  lattice there is some  $\beta = \beta_c$  ( $5.2 \leq \beta_c \leq 5.3$ ) at which the charged pion condensate evaporates. This transition appears to be first order. Such first order behaviour was predicted for  $\mu_I$  large enough by Son and Stephanov [2] who argued that at high  $\mu_I$  the fermions would effectively decouple, and the phase transition would be that for pure glue, which is known to be first order. We note from our observations that the situation is not quite this simple. The pure glue transition on an  $N_t = 4$  lattice occurs at  $\beta \approx 5.7$  [10, 11]. Since our observations place  $\beta_c$  somewhat lower than this, and close to the value of the  $\mu_I = 0$  finite temperature transition, the quarks *are* having an effect. We also note that Son and Stephanov suggest that the first order deconfinement transition at high temperature is distinct from the  $I_3$  symmetry restoring transition. Our evidence is that these 2 transitions are coincident. This means that the second order segment of the phase boundary can be considered as driven purely by the chemical potential, which makes their argument for  $O(2)$  universality less compelling. We note that, in our paper on 2-colour QCD at finite  $\mu$  and  $T$  [7], we present an alternative argument for the first-order finite-temperature transition which that theory exhibits for large  $\mu$ .

In addition, we have simulated our  $N_t = 4$  system at fixed  $\beta$ , varying  $\mu_I$ . In particular we have performed simulations at  $\beta = 4.0$  which is at near-zero temperature, and  $\beta = 5.0$  where the system is clearly at a finite temperature. Both of these simulations showed a second order transition. Not surprisingly, the scaling close to this transition appeared tricritical, which we again interpret as a coarse-lattice artifact.

We have noted throughout this paper the similarity between 3-colour QCD at finite  $\mu_I$  and 2-colour QCD at finite quark-number chemical potential,  $\mu$ . The correspondence is seen by identifying  $\frac{1}{2}\mu_I$  with  $\mu$ , the charged pion condensate with the diquark condensate and the isospin density with the quark number density. This similarity is seen both in simulations and in effective Lagrangian analyses. The expected position of the zero temperature transition is the same  $\mu_I = m_\pi$  ( $\mu = \frac{1}{2}m_\pi$ ). Its nature – second order with mean-field exponents is believed to be the same. In both systems the spontaneous symmetry breaking is in the Goldstone mode (superfluid). At finite temperature the condensate evaporates at

a transition which is first order for  $\mu_I$  ( $\mu$ ) large enough. This line of first order transitions softens to second order and the line of second order transitions connects to the zero temperature transition. Thus, we can use 2-colour QCD results at finite  $\mu$  as a guide as to QCD at finite  $\mu_I$ .

We are extending these simulations to a larger lattice ( $12^3 \times 24$ ) and weaker coupling where we hope to observe the expected mean-field transition, and rule out the  $O(2)$  alternative. This lattice will also enable us to measure the spectrum of Goldstone and pseudo-Goldstone excitations as functions of  $\mu_I$ . More extensive spectrum analyses at  $\mu_I = 0$  will give us a more definitive scale for these phenomena, in addition to a value for  $m_\pi$  with which to compare  $\mu_c$ . Configurations will be stored so that we can make other spectroscopy measurements at finite  $\mu_I$ . We will also extend the finite temperature simulations to a  $12^3 \times 6$  lattice since it is difficult to determine the order of the continuum transitions from  $8^3 \times 4$  lattices. In addition we will study the instantons at large  $\mu_I$  since it is believed that instantons and their interactions have a relatively simple structure at large isospin density, analogous to what has been predicted for large quark-number density [12].

We are also starting lattice QCD simulations including both a chemical potential  $\mu_I$  for isospin and a chemical potential  $\mu_s$  for strangeness. Here effective Lagrangian analyses have indicated that there is a competition between the formation of pion and kaon condensates as  $\mu_I$  and  $\mu_s$  are varied independently and that the boundary between the region with a pion condensate and that with a kaon condensate is a line of first order transitions [13].

Although our simulations have been limited to zero baryon number density, it is interesting to know how much of this analysis is relevant to systems with finite baryon number density and isospin density. If it does have relevance, charged pion condensates could contribute to the equation-of-state of nuclear matter and thus be important in understanding the physics of neutron stars and perhaps large nuclei.

### Acknowledgements

DKS was supported by DOE contract W-31-109-ENG-38. JBK was supported in part by an NSF grant NSF PHY-0102409. JBK wishes to thank D. Toublan for many useful discussions. DKS would like to thank R. Pisarski for emphasizing the importance of

extracting pressure and energy density.

- 
- [1] J. B. Kogut and D. K. Sinclair, Nucl. Phys. B(Proc. Suppl.) 106 (2002).
  - [2] D. T. Son and M. A. Stephanov, Phys. Rev. Lett. 86, 592 (2001); D. T. Son and M. A. Stephanov, Yad. Fiz. 64, 899 (2001), Phys. Atom. Nucl. 64, 834 (2001).
  - [3] J. B. Kogut and D. K. Sinclair, eprint hep-lat/0201017 (2002). S. Gupta, eprint hep-lat/0202005 (2002).
  - [4] S. Hands, J. B. Kogut, M.-P. Lombardo and S. E. Morrison, Nucl. Phys. B558, 327 (1999); J. B. Kogut, D. K. Sinclair, S. J. Hands and S. E. Morrison, Phys. Rev. D64, 094505 (2001); R. Aloisio, V. Azcoiti, G. Di Carlo, A. Galante and A. F. Grillo, Phys. Lett. B493, 189 (2000); R. Aloisio, V. Azcoiti, G. Di Carlo, A. Galante and A. F. Grillo, Nucl. Phys. B606, 322 (2001); A. Nakamura, Phys. Lett. 149B, 391 (1984); S. Muroya, A. Nakamura and C. Nonaka, eprint nucl-th/0111082 (2001).
  - [5] J. B. Kogut, D. Toublan and D. K. Sinclair, Argonne preprint ANL-HEP-PR-02-005 (2002).
  - [6] J. B. Kogut, M. A. Stephanov and D. Toublan, Phys. Lett. B464, 183 (1999); J. B. Kogut, M. A. Stephanov, D. Toublan, J. J. M. Verbaarschot and A. Zhitnitsky, Nucl. Phys. B582, 477 (2000).
  - [7] J. B. Kogut, D. Toublan and D. K. Sinclair, Phys. Lett B514, 77 (2001);
  - [8] I. D. Lawrie and S. Sarbach, in *Phase Transitions and Critical Phenomena, Volume 9* (Academic Press, London, 034508).
  - [9] K. Splittorff, D. Toublan and J. J. M. Verbaarschot, Nucl. Phys. B620, 290 (2002).
  - [10] F. R. Brown, et al., Phys. Rev. Lett. 61, 2058 (1988).
  - [11] P. Bacilieri, et al., Phys. Rev. Lett. 61, 1545 (1988).
  - [12] D. T. Son, M. A. Stephanov and A. R. Zhitnitsky, Phys. Lett. B510, 167 (2001).
  - [13] J. B. Kogut and D. Toublan, Phys. Rev. D64, 034007 (2001).